A fast and sensitive method for the continuous in situ determination of dissolved methane and its δ 13 C-isotope ratio in surface waters

10 authors, including:

Jan F Hartmann
Universität Heidelberg
5 PUBLICATIONS   **6** CITATIONS

SEE PROFILE

Gentz Torben
Alfred Wegener Institute Helmholtz Centre for Polar and Marine R...
17 PUBLICATIONS   **149** CITATIONS

SEE PROFILE

Markus Greule
Universität Heidelberg
59 PUBLICATIONS   **507** CITATIONS

SEE PROFILE

Hans-Peter Grossart
Leibniz-Institute of Freshwater Ecology and Inland Fisheries
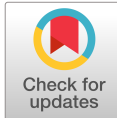**490** PUBLICATIONS   **8,704** CITATIONS

SEE PROFILE

Some of the authors of this publication are also working on these related projects:

Structural and functional studies on outer membrane vesicles of bacteria View project

Eukaryotic colonization of microplastics in aquatic environments View project

A fast and sensitive method for the continuous in situ determination of dissolved methane and its δ^{13}C-isotope ratio in surface waters

Jan F. Hartmann [ORCID],[1]* Torben Gentz,[2] Amanda Schiller,[1] Markus Greule,[1] Hans-Peter Grossart [ORCID],[3,4]
Danny Ionescu,[3] Frank Keppler,[1] Karla Martinez-Cruz,[3] Armando Sepulveda-Jauregui,[3]
Margot Isenbeck-Schröter[1]

[1]Institute of Earth Sciences, Heidelberg University, Heidelberg, Germany
[2]Alfred-Wegener Institute, Helmholtz Centre for Polar and Marine Research, Bremerhaven, Germany
[3]Department of Experimental Limnology, Leibniz-Institute of Freshwater Ecology and Inland Fisheries, Stechlin, Germany
[4]Institute of Biochemistry and Biology, Potsdam University, Potsdam, Germany

Abstract

A fast and sensitive method for the continuous determination of methane (CH_4) and its stable carbon isotopic values (δ^{13}C-CH_4) in surface waters was developed by applying a vacuum to a gas/liquid exchange membrane and measuring the extracted gases by a portable cavity ring-down spectroscopy analyser (M-CRDS). The M-CRDS was calibrated and characterized for CH_4 concentration and δ^{13}C-CH_4 with synthetic water standards. The detection limit of the M-CRDS for the simultaneous determination of CH_4 and δ^{13}C-CH_4 is 3.6 nmol L^{-1} CH_4. A measurement precision of CH_4 concentrations and δ^{13}C-CH_4 in the range of 1.1%, respectively, 1.7‰ (1σ) and accuracy (1.3%, respectively, 0.8‰ [1σ]) was achieved for single measurements and averaging times of 10 min. The response time τ of 57 ± 5 s allow determination of δ^{13}C-CH_4 values more than twice as fast than other methods. The demonstrated M-CRDS method was applied and tested for Lake Stechlin (Germany) and compared with the headspace-gas chromatography and fast membrane CH_4 concentration methods. Maximum CH_4 concentrations (577 nmol L^{-1}) and lightest δ^{13}C-CH_4 ($-35.2‰$) were found around the thermocline in depth profile measurements. The M-CRDS-method was in good agreement with other methods. Temporal variations in CH_4 concentration and δ^{13}C-CH_4 obtained in 24 h measurements indicate either local methane production/oxidation or physical variations in the thermocline. Therefore, these results illustrate the need of fast and sensitive analyses to achieve a better understanding of different mechanisms and pathways of CH_4 formation in aquatic environments.

It has been a primary task of climate research ever since the 1950s to evaluate the impact of greenhouse gases, such as methane (CH_4), in the atmosphere, the world's oceans, sea ice, and glaciers (Revelle and Suess 1957; Forster et al. 2007). However, local and global quantification of dissolved CH_4 in aquatic systems and total emissions to the atmosphere in marine, limnic, and fluvial systems is highly complex and yet holds large uncertainties (Reeburgh 2007; Bastviken et al. 2011; Saunois et al. 2016).

In aquatic environments, CH_4 originates from biogenic (e.g., by methanogenic archaea) and abiogenic/thermogenic sources (e.g., hydrothermalism), both showing distinct stable carbon isotope values ranging from $-55‰$ to $-70‰$ and $-25‰$ to $-55‰$, respectively (e.g., Schoell 1988; Kirschke et al. 2013). Biogenic CH_4 in aquatic systems has been suggested to be mainly controlled by production by methanogens and oxidation by methanotrophs (Thauer et al. 2008; Tranvik et al. 2009; Oswald et al. 2015). Traditionally, it has been believed that methanogenesis occurs primarily in anoxic environments, such as natural wetlands and rice paddies, freshwater reservoirs, lakes, rivers, and organic waste deposits (Mah et al. 1977; Reeburgh 2013). The flux of CH_4 from these environments to the atmosphere has been often studied (Bastviken et al. 2011; Ortiz-Llorente and Alvarez-Cobelas 2012; Holgerson and Raymond 2016; Wik et al. 2016). Additionally, studies of dissolved CH_4 profiles of the oceanic water column show supersaturated concentrations (compared to the atmosphere) in well oxygenated surface layers (ca. 100–300 m) (e.g., Brooks and Sackett 1973; Lamontagne et al. 1973, 1974; Burke et al. 1988), in which CH_4 is strongly suggested to stem from a biological source,

*Correspondence: Jan.Hartmann@geow.uni-heidelberg.de

contributing around 4% of the atmospheric CH_4. Recently, it has been also shown that CH_4 is produced in continental oxic waters by different microbial processes (Grossart et al. 2011; Tang et al. 2016). Consequently, CH_4 emissions to the atmosphere derived from oxic surface inland waters might be underestimated in the global CH_4 budget (Tang et al. 2016). Recent studies highlight the presence of methane formation in oxygenated freshwater and marine surface waters (e.g., Grossart et al. 2011; Tang et al. 2014; Repeta et al. 2016), and it has been suggested that algae per se might produce CH_4 under aerobic conditions by a hitherto unknown mechanism (Lenhart et al. 2015). The various mechanisms and pathways of CH_4 transformation as well as hydrological mixing processes can be characterized and distinguished by the determination of $\delta^{13}C$-CH_4 in water (Sansone et al. 1999; Maher et al. 2015). A fast, sensitive, and continuously measuring method to determine in situ both CH_4 concentration and $\delta^{13}C$-CH_4 values in water environments is therefore desirable when addressing the complex microbial pathways and transformations of CH_4 in aquatic ecosystems.

For decades, CH_4 analyses were mainly based on the collection of discrete water samples, followed by gas-extraction via the headspace technique and analysis in the laboratory after field work (Kampbell et al. 1989; Bange et al. 1994; Snow and Slack 2002; Bussmann et al. 2013; Tang et al. 2014). Thereby, the temporal and spatial resolution of mechanisms controlling CH_4 distribution in the aquatic systems was strongly limited by the number of samples. First studies presenting simultaneous data for dissolved CH_4 and $\delta^{13}C$-CH_4 in aquatic systems are based on the spray chamber-method (Gülzow et al. 2013; Maher et al. 2015). However, those methods are suitable for long term measurements only, as the spray chamber-method is based on the gas-equilibrium between water and analyzed headspace, leading to measurement times of several minutes to hours (Webb et al. 2016). Recently, fast in situ methods for the determination of dissolved CH_4, such as underwater mass spectrometry (UWMS) and a membrane contactor for gas/liquid exchange coupled with an off-axis integrated cavity output spectrometer (M-ICOS) were introduced by, e.g., Schlüter and Gentz (2008) and Gonzalez-Valencia et al (2014), respectively, but are limited to CH_4 concentration only. Wankel et al. (2013) further improved UWMS by developing a near real-time analyser for $\delta^{13}C$-CH_4 measurements in the deep ocean. However, this analyser can only be used in environments with CH_4 values above 0.1 mmol L^{-1} and 0.5 mmol L^{-1} for the determination of CH_4 concentration and $\delta^{13}C$-CH_4 values, respectively; concentrations which occur, for example, at/in hydrothermal vents/systems or cold seeps (e.g., Dando et al. 1995; Botz et al. 1999).

Thus, for surface waters and shallow freshwater environments with low CH_4 concentrations, methods to determine short term $\delta^{13}C$-CH_4 variations would offer a better understanding of the different pathways, sources, and sinks of

CH_4 and, consequently, help to improve the global CH_4 budget. We developed a sensitive, fast, and continuous method for the determination of CH_4 concentration and $\delta^{13}C$-CH_4 values in natural waters with concentrations in the *n*-molar to μ-molar range.

In a first step, we demonstrate the validation of our measurement setup, a portable cavity ring-down spectroscopy analyser (CRDS) in combination with a gas/liquid exchange membrane (M)—collectively called "M-CRDS"—in vacuum mode. The method was compared via laboratory experiments and cross-check measurements to gas chromatography-flame ionization detection (GC-FID) and gas chromatography-combustion-isotope ratio mass spectrometry (GC-C-IRMS). We further present simultaneous field measurements of CH_4 concentration and $\delta^{13}C$-CH_4 values in Lake Stechlin, Germany, providing new insights into the origin and fate of CH_4 in aquatic environments.

Methods and procedures

Membrane-coupled CRDS-system

The experimental setup for continuous and simultaneous measurements of CH_4 concentration and $\delta^{13}C$-CH_4 values in water is shown in Fig. 1. The major parts are indicated by capital letters (A–K). The setup can be subdivided into a water and a gas system. The water system mainly contains a pump and filtering units as well as the membrane contactor. The gas system consists of a vacuum pump, a dilution chamber, and the CRDS analyser (G2201-i of Picarro, U.S.A.). The M-CRDS is built as a modular structured system, allowing a quick replacement of individual pieces, as all parts are easily exchangeable within minutes. Due to the compact and robust construction, the M-CRDS is absolutely suitable for applications in the field or on, e.g., ship-expeditions.

In the water system, the water flow is generated by a submersible pump (Part A, MP1, Grundfoss, Denmark) and filtered by different filtering units (Part B, Infiltec, Germany) of decreasing mesh sizes of 200 μm, 100 μm, 25 μm, and/or 5 μm. The mesh sizes depend on the requirements of the particular sampled aquatic system to ensure longevity of the measuring setup. Several sensors log in situ water temperature (°C) at the submersible pump as well as water temperature (°C) at the membrane, redox potential (V), pH, O_2 (%), and conductivity (S m^{-1}) in a bypass (Part C, WTW, Germany). Samples for reference measurements during laboratory experiments were also taken from that bypass.

Dissolved CH_4 is extracted by a membrane contactor (Part E, LIQUI-CEL mini module®, 3M Industrial Group, U.S.A.) as described by Noble and Stern (1995). The water flow through the membrane contactor is adjusted by a high quality mass flow controller (Part D, Analyt-MTC series 358, Germany) to 500 ± 5 mL min^{-1} to achieve best response times The flow rate, and consequentially the response time, is generally limited by the membrane contactor to 500 mL min^{-1} as higher
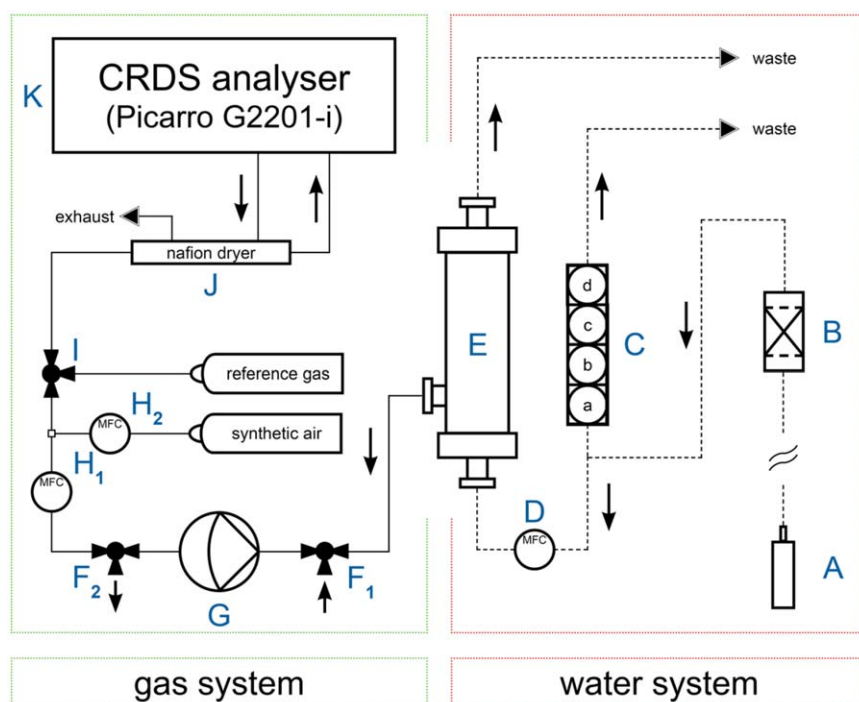
Fig. 1. Schematic overview of the CRDS analyser combined with a membrane contactor (collectively called M-CRDS) setup for continuous and simultaneous determination of dissolved CH_4 concentration and δ^{13}C-CH_4 in water. In the water system, water is pumped by a submersible pump (A), filtered (B), and analyzed by several sensors in a bypass (C). Main water flow is adjusted by a mass flow controller (D) and directed to the membrane contactor (E). In the gas system part, gases are extracted by the membrane pump (G). The vacuum pump and tubes are flushed via two automatic three-way-valves (Part F_1 and F_2) with ambient air avoiding condensation in the system. Depending on the CH_4 concentration, the gas sample can be diluted with synthetic air by two mass flow controllers (H_1 for gas sample flow and H_2 for synthetic air flow). Reference gases for calibration prior, during and following the experiments are introduced via three-way-valves (I). Gases are dried by a Nafion drying tube (J) prior to analysis by the CRDS analyser (K).

water flow rates might deform the pores due to increased hydrostatic pressure, which results in decreasing gas exchange through the membrane (Boulart et al. 2010; Wankel et al. 2013). The membrane contactor is set to a vertical position and the flow enters the bottom and exits the top to assure a bubble-free water-air-boundary at the membrane surface.

In the gas system, vacuum is applied to the membrane contactor using a membrane pump (Part G, N920KT.29.18, KNF, Germany) to minimize equilibration times for gas exchange between water and the analyzed headspace. The flow rate of extracted gas is $\sim$ 50 mL min^{-1}. Even though the membranes are hydrophobic with small pores, water vapor is removed by the vacuum mode (up to 5%). Therefore, the vacuum pump and tubes are flushed via two automatic three-way-valves (Part F_1 and F_2) with ambient air for 7 min (every 4 h) avoiding condensation in the system and guaranteeing a constant vacuum.

As the CRDS' operational range is limited to a maximum concentration of 1000 ppm, a small-sized dilution chamber was applied to dilute highly concentrated sampling gases with synthetic air (20.5 ± 0.5 mol% O_2 in N_2, AirLiquide, Germany). The dilution is regulated via two high quality mass flow controllers (Parts H_1 [up to 5 mL min^{-1}] and H_2

[up to 500 mL min^{-1}], Analyt-MTC series 358, Germany) in a concentration-depended manner. Reference gases for prior calibration, during and following the experiments are introduced via three-way-valves (Part I, Swagelok, Germany). Since all gas samples are dried by a Nafion® drying tube (Nafion MD110, PermaPure LLC, U.S.A.) before measurements to ensure higher accuracy (Part J), water vapor concentrations are less than 0.2% in the analyser, where the software internal water correction algorithm shows its best applicability (Rella et al. 2013). Gases are subsequently directed to the portable CRDS analyser and analyzed for CH_4 concentration and δ^{13}C-CH_4 (Part K). The Picarro® G2201-i measures $^{12}CH_4$, $^{13}CH_4$, and H_2O individually and quasi-simultaneously at a very high temporal resolution (1 Hz) and provides δ^{13}C values in ‰ relative to the Vienna Pee Dee Belemnite standard (V-PDB). Picarro® uses built-in pressure and temperature control systems as well as automatic water vapor correction to ensure a high stability of its portable analyser. Effects of water vapor on the measurement were corrected automatically by the Picarro® software. The manufacturer states concentration precision for the analysis of CH_4 in the "high precision mode" of 5 ppbv $\pm$ 0.05% (^{12}C) and 1 ppbv $\pm$ 0.05% (^{13}C), while a concentration range from 1.8 ppm to 12 ppm is covered. The given precision of

$\delta^{13}C$-CH_4 is < 0.8‰. During all measurements, the analyser was operated in a Zargesbox with built-in venting system and uninterruptible power supply system to ensure a continuous operation during the measurements.

Method calibration

Data obtained by the M-CRDS cannot be corrected by headspace calculations since the extraction of CH_4 from the water is based on the application of a vacuum. Therefore, the M-CRDS is calibrated for CH_4 concentration using synthetic water standards including CH_4 at certain concentrations (SubSeaSpec UG, Germany) as described by Schlüter and Gentz (2008). For this approach, several 60 L water reservoirs were filled with tap water and continuously flushed with reference gas. Each reservoir was flushed with different CH_4 concentration (5 ppm, 100 ppm, and 1000 ppm CH_4 in methane-free synthetic air, AirLiquide, Germany) and pumped to the membrane contactor subsequently as described in Fig. 1. A multi-channel pump was used to generate samples of different CH_4 concentrations through mixing of standard water from the water reservoirs and methane-free synthetic air (20 mol% O_2 in N_2, AirLiquide, Germany) flushed tap water (zero water). In order to quality assure the $\delta^{13}C$-CH_4 values, water samples from lakes, ponds as well as groundwater with different stable carbon isotopic values were measured both by M-CDRS and GC-C-IRMS since certified aquatic $\delta^{13}C$-CH_4 standards are not yet available. All values were averaged over 10 min measurement interval.

Method characterization

Measuring accuracy, precision, and the response time for the simultaneous determination of the concentration and $\delta^{13}C$-CH_4 in water were validated via measuring water reservoirs and water sampling bags with constant CH_4 concentration and $\delta^{13}C$-CH_4 values by M-CRDS, GC-FID and GC-C-IRMS. The response time of the M-CRDS was assessed by switching between two water reservoirs with different CH_4 concentrations and $\delta^{13}C$-CH_4 for low to high and high to low concentration transitions (Johnson 1999; Webb et al. 2016). The response time is given as the time constant τ of exponential decay during the concentration transitions using Eq. 1 (Johnson 1999).

$$C = A + B \; e^{\frac{-t}{\tau}} \tag{1}$$

where C is the gas phase from the membrane contactor, t is time (s), and A, B, and τ are constants found for each fit. Although this model is mainly used for equilibration devices (Johnson 1999), the time constant τ is a primary factor to evaluate the performance of the devices during maximum to minimum and minimum to maximum transitions.

Since CH_4 measurements by CRDS are dependent on the air composition of the sampled gas (Nara et al. 2012), tests were conducted to examine the effects of O_2 in the sampling

gas on the measurement of CH_4 concentration. Therefore, the extracted air was analyzed for O_2 concentration by an optical oxygen sensor (FiBox 4, PreSense, Germany). Gas solubility is highly temperature dependent. Therefore, the impact of changes in the water temperature within the tubing on the membrane properties was examined, using a water reservoir (200 L) at constant temperature, CH_4 concentration and ^{13}C-CH_4. The tubing was heated using a water-bath with temperature control and both in situ temperatures at the membrane and at the submersible pump were measured to examine the warming of the water in the tubes.

GC-FID and GC-C-IRMS measurements

Subsamples of the water mixtures of different CH_4 concentrations (4 nmol L^{-1} CH_4 to 500 nmol L^{-1} CH_4) were independently measured in the laboratories of the University of Heidelberg, Germany and the Alfred-Wegener Institute (AWI), Helmholtz Centre for Polar and Marine Research located in Bremerhaven (Germany) via the headspace technique (Kampbell et al. 1989) by gas chromatography (GC-FID, ThermoFinnigan, Waltham, U.S.A.) and stable isotope ratio mass spectrometry (GC-C-IRMS, Delta^{plus} XL, Thermo Finnigan, Bremen, Germany) analyses.

The CH_4 concentration and $\delta^{13}CH_4$ ratios in water samples were measured using 255 mL serum vials, closed with butyl rubber stoppers and aluminum crimp caps. Each serum vial was shaken vigorously for 120 s to reach equilibration between the water and the gas headspace. Promptly, CH_4 concentration in the headspace was measured by GC-FID and CH_4 concentration in the water determined using Henry's law (Wiesenburg and Guinasso 1979) and solubility coefficients for CH_4 according to Weiss (1974) and Yamamoto et al. (1976).

Prior to this study, the $\delta^{13}C$-CH_4 ratios for several environmental samples were determined by GC-C-IRMS for calibration purposes. Interfering compounds were separated by GC and CH_4 trapped on Hayesep D. The sample was then transferred to the IRMS system (ThermoFinnigan Delta^{plus} XL, Thermo Finnigan, Bremen, Germany) via an open split. The working reference gas was carbon dioxide of high purity (carbon dioxide 4.5, Messer Griesheim, Frankfurt, Germany) with a known $\delta^{13}C$ value of -23.634 ± 0.006‰ vs. V-PDB (calibrated at MPI for Biogeochemistry in Jena, Germany). All $\delta^{13}C$-CH_4 values were corrected using two CH_4 working standards (isometric instruments, Victoria, Canada). The known $\delta^{13}C$-CH_4 values of the two working standards in ‰ vs. V-PDB were -23.9 ± 0.2 and -54.5 ± 0.2. All samples were normalized by two-scale anchor calibration according to Paul et al. (2007) and show an average standard deviation of the analytical measurements in the range of 0.1–0.3‰.

Field application at Lake Stechlin

The M-CRDS was applied and tested for suitability during field work at Lake Stechlin (Germany) in July/August 2015. Lake Stechlin is a dimictic meso-oligotrophic lake ca. 80 km
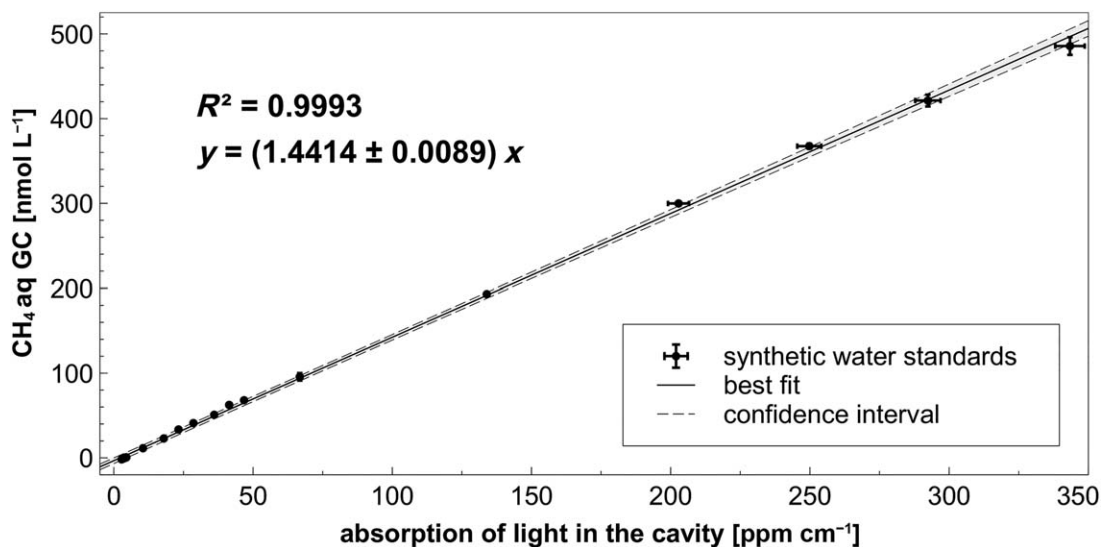
Fig. 2. The results of the calibration of the M-CRDS for CH_4 concentration using synthetic water standards ($n = 21$). Error bars (1σ) of measurements mainly lie within symbols and reflect the noise within the measurement interval (10 min). Best fit was calculated by geometric mean regression (Sokal and Rohlf 1995).

northeast of Berlin, Germany. The M-CRDS was deployed from a large platform that is constantly installed in the lake (LakeLab: http://www.lake-lab.de). Vertical CH_4 concentration profiles through the entire water column were measured with the M-CRDS setup. To verify the applicability of the system for field application, the same CH_4 profiles were measured quasi-simultaneously at the LakeLab by the M-CRDS, a membrane contactor for gas/liquid exchange coupled with an off-axis integrated cavity output spectrometer (M-ICOS) (Gonzalez-Valencia et al. 2014), and with a GC-FID (Shimadzu, Japan) in the laboratory (Grossart et al. 2011). The M-ICOS system was calibrated and operated according to Gonzalez-Valencia et al. (2014). Samples for GC-FID analyses were independently sampled by a hydrocast and measured immediately thereafter (1–2 h) in the laboratories of the Leibniz-Institute of Freshwater Ecology and Inland Fisheries (IGB, Germany) via the headspace technique (Kampbell et al. 1989). The working reference gas for CH_4 was analyzed prior and at the end of the profile measurements.

Based on the results of the vertical CH_4 concentration profiles, subsequent 24-h measurements were performed at the depth of maximum CH_4 concentration in the oxic water column at the LakeLab. The working reference gas for CH_4 (5 ppm CH_4 and 500 ppm CO_2 in synthetic air) was analyzed every 8 h during the measurements. Water flow was regulated to a constant flow of 500 ± 5 mL min^{-1} all time.

Isotope source signatures were determined using keeling plot analyses (Keeling 1958). The keeling plot of the isotopic composition (‰) vs. the inverse concentration 1/CH_4 (L nmol^{-1}) of the analyzed samples provides the isotope ratio of the CH_4 source. The extrapolated intercept of the straight line in the Keeling plot (Sokal and Rohlf 1995) corresponds to the situation when the concentration is very high and dominated by CH_4 (1/$CH_4 = 0$) and thus reveals the isotope ratio of the CH_4 source. For a detailed discussion of the Keeling plot method for environmental applications, please refer to Keppler et al. (2016) and Pataki et al. (2003).

Results and discussion

Method calibration

The calibration results of the M-CRDS using synthetic CH_4-water standards (water enriched with CH_4) are shown in Fig. 2. Concentration data was averaged over the 10-min measurement interval. The CH_4 measured by the M-CRDS setup (ppm cm^{-1}) and the dissolved CH_4 concentrations gained by the well-established GC-FID analysis are highly correlated ($R^2 = 0.9993$). The concentration of dissolved CH_4 can be derived from the obtained data of the M-CRDS setup via the linear best fit function $y = 1.4414x$ (Fig. 2).

Analyses of δ^{13}C-CH_4 values in the synthetic water standards as well as in the reference gases, used to produce those standards, show nearly identical and constant isotopic values. Due to a lack of aquatic δ^{13}C-CH_4 reference standards, water samples from lakes, ponds as well as groundwater with different stable carbon isotopic values were measured both by M-CDRS and GC-C-IRMS (Fig. 3). The mean offset between the δ^{13}C-CH_4 values measured by the M-CRDS and the GC-C-IRMS is 0.5 ± 1.1‰. Isotopic values were averaged over the 10-min measurement interval. The results show that stable carbon isotope fractionation during water-gas transfer in the membrane contactor was not observed and can therefore be excluded.
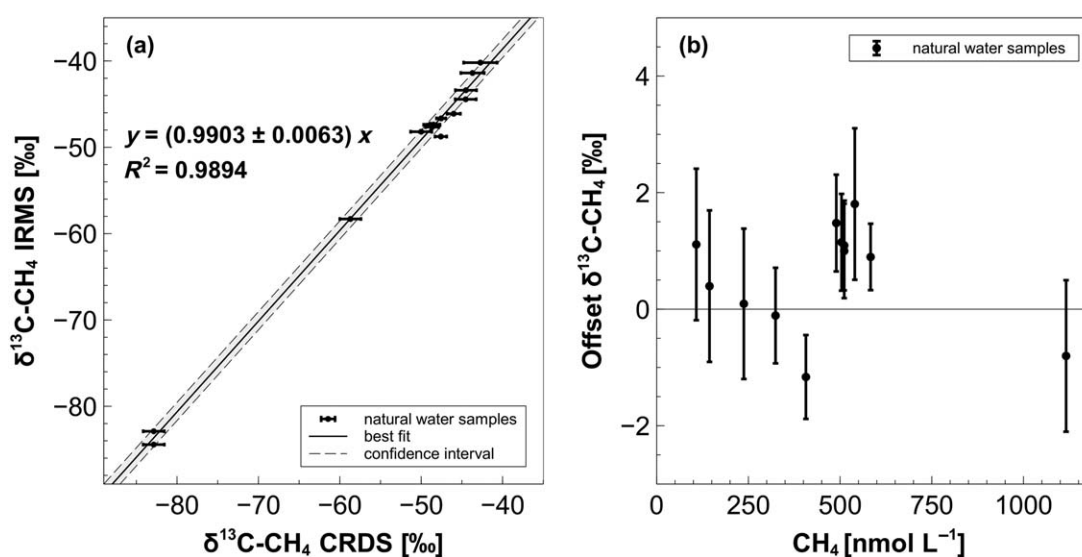
Fig. 3. The δ^{13}C-CH$_4$ values of natural water samples ($n = 15$) with different stable carbon isotopic values measured both by M-CDRS and GC-C-IRMS (**a**). Error bars (1σ) of measurements reflect the noise within the measurement interval (10 min). Best fit was calculated by geometric mean regression (Sokal and Rohlf 1995). Offset of δ^{13}C-CH$_4$ values for natural water samples ($n = 15$) with different δ^{13}C-CH$_4$ values and CH$_4$ concentration were measured by M-CRDS in comparison with GC-C-IRMS (**b**).

Table 1. Results of the characterization of the M-CRDS for CH$_4$ concentration and δ^{13}C-CH$_4$.

Measurement parameters	Values
CH$_4$ detection limit (for the simultaneous determination of CH$_4$ and δ^{13}C-CH$_4$)	3.6 nmol L^{-1}
Response time τ (continuous mode)	57 ± 5 s
Measuring precision (CH$_4$) (1σ)	1.1%
Measuring accuracy (CH$_4$)	1.3%
Measuring precision (δ^{13}C-CH$_4$) (1σ)	1.7‰
Measuring accuracy (δ^{13}C-CH$_4$)	0.8‰

Method characterization

All laboratory tests performed suggest that the M-CRDS setup is a sensitive and fast method, suitable for the simultaneous determination of dissolved CH$_4$ concentration and δ^{13}C-CH$_4$ values in water. Determined measurement parameters are given in Table 1.

The detection limit for the simultaneous determination of CH$_4$ and δ^{13}C-CH$_4$ values is 3.6 nmol L^{-1} CH$_4$, which is significantly lower than reported CH$_4$ concentrations in many freshwater environments (Abril and Iversen 2002; Juutinen et al. 2009; Grossart et al. 2011; Bussmann et al. 2013). The measuring accuracy of the M-CRDS for CH$_4$ concentration and δ^{13}C-CH$_4$ values is 1.3% and 0.8‰, respectively ($n = 20$). The precision (1σ) is 1.1% for CH$_4$ concentration and 1.7‰ for δ^{13}C-CH$_4$ ($n = 20$) compared to the validation by GC-FID and GC-C-IRMS since certified aquatic CH$_4$ and δ^{13}C-CH$_4$ standards are not available. The precision of δ^{13}C-CH$_4$ values increases with increasing CH$_4$ concentrations from less

than 1.5‰ for CH$_4$ concentrations <250 nmol L^{-1} to 0.5‰ (> 600 nmol L^{-1}). The mean difference of δ^{13}C-CH$_4$ values determined by the M-CRDS and the GC-C-IRMS is $0.76 \pm 1.19‰$. All samples were measured for at least 15 min to achieve stable measured values and have been averaged over 10 min.

In addition, response times τ for the simultaneous determination of CH$_4$ concentration and δ^{13}C-CH$_4$ values were calculated according to Johnson (1999) and show an average value of 57 ± 5 s ($n = 8$) for both ^{12}CH$_4$ and ^{13}CH$_4$ for surface waters (Fig. 4). A concentration dependence of the determined response time was not observed. A detailed discussion of response times τ for air–water equilibration devices is presented in Webb et al. (2016).

The response time for determination of CH$_4$ and δ^{13}C-CH$_4$ in water with "conventional" equilibration devices is generally based on Henry's law, establishing the equilibrium between water and the analyzed headspace. Consequentially, response times for concentration transitions in equilibration devices are increased by long equilibration times for CH$_4$ due to the lower solubility of CH$_4$ in water. Isotopic values are further affected by isotopic mixing, which requires complete equilibration between water and headspace (Faure 1986; Webb et al. 2016).

The M-CRDS avoids the occurrences of long equilibration times for CH$_4$ as well as memory and isotopic mixing effects occurring with "conventional" equilibration devices. The system extracts the analyzed gases by a vacuum and therefore eliminates the time-consuming establishment of the equilibrium between water and analyzed headspace. As a consequence, the M-CRDS provides more than two times

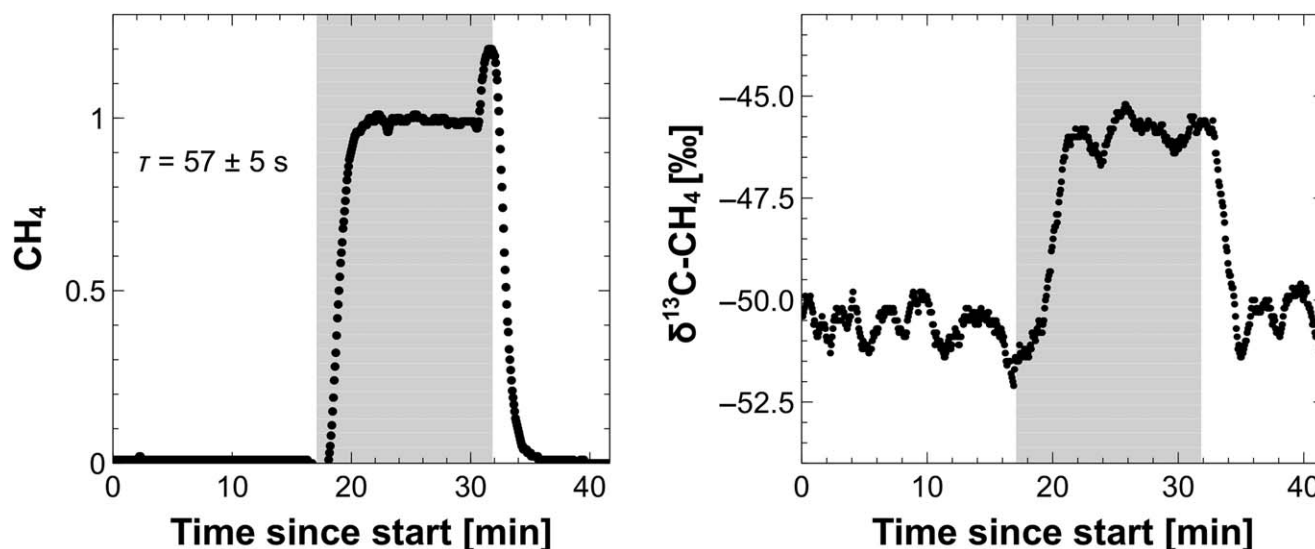**Fig. 4.** Exemplary response time of CH_4 concentration and δ^{13}C-CH_4 values for low to high and high to low concentration transitions. Concentrations are normalized to 0 (1st reservoir, 130 nmol L^{-1}) and 1 (2nd reservoir, 170 nmol L^{-1}). Response times of the M-CRDS were assessed by the calculation of the time constant τ (s) (Johnson 1999) ($n = 8$). δ^{13}C-CH_4 data has been smoothed to 30 s averaging interval. High concentration measurement marked in gray. Spikes in CH_4 concentration arise from increased retention time of waters in the membrane contactor due to switching between water reservoirs.

Table 2. Comparison of response times for the simultaneous determination of CH_4 and δ^{13}C-CH_4 in water from other studies for different devices (after Webb et al. 2016) compared with response times calculated for the M-CRDS (this study).

Device	Response time τ (s)	Study
Weiss-type (small)	2248	Li et al. (2015)
General oceanics	2041 ± 247	Webb et al. (2016)
Shower head	1657 ± 69	Webb et al. (2016)
Weiss-type (large)	1200	Rhee et al. (2009)
Marble	893 ± 12	Webb et al. (2016)
Bubble-type	678	Gülzow et al. (2011)
Liqui-Cel (medium)	417 ± 126	Webb et al. (2016)
Liqui-Cel (small)	177 ± 126	Webb et al. (2016)
Liqui-Cel (large)	117 ± 6	Webb et al. (2016)
Liqui-Cel (small) in vacuum mode	57 ± 5	This study

faster analyses for the simultaneous determination of CH_4 concentration and δ^{13}C-CH_4 values compared to previously published methods (Rhee et al. 2009; Gülzow et al. 2013; Li et al. 2015; Webb et al. 2016) (Table 2) and, more importantly, shows identical response times for low to high and high to low concentration transitions, whereas significant equilibration delays for δ^{13}C-CH_4 values occur for "conventional" air–water equilibration devices for transitions from high to low concentration levels due to isotope mixing effects (Faure 1986; Webb et al. 2016). These improvements show that the M-CRDS response times are

mainly limited by the rise/fall-time of the CRDS analyser due to the more demanding isotopic measurement rather than the gas-extraction step.

Since gas solubilities as well as the extraction by the membranes are highly temperature dependent, the impact of changes in the water temperature on the membrane properties was examined. The temperature difference between the in situ water temperature at the membrane and the temperature at the submersible pump was examined for a range of 0–12°C. The observed temperature dependency for the measurements was weak ($R^2 = 0.3132$) and insignificant compared to the measuring accuracy and precision of 1.3% and 1.1%, respectively. Significant effects of temperature differences (e.g., due to warming of the water in the tubing) on the analyzed CH_4 concentration and/or extraction efficiency can therefore be neglected for surface waters and moderate climates.

Nara et al. (2012) showed potential interferences of the extracted gas matrix on the CH_4 concentration and δ^{13}C-CH_4 measurements by the CRDS. Hence, we examined the effects of the oxygen concentration in the extracted air. Changes in aquatic O_2 saturation of approximately 80% result in a change in O_2 excess concentration in the extracted air of up to 8000 ppm. Nara et al. (2012) show resulting pressure-broadening effects on CH_4 measurements for ambient air concentrations, which is significant lower than the measuring accuracy and precision (1.3% and 1.1%, respectively) of the M-CRDS and no significant isotopic bias for ^{13}C-CH_4 measurements by CRDS analysis. The natural samples used for the δ^{13}C-CH_4 calibration/validation of the
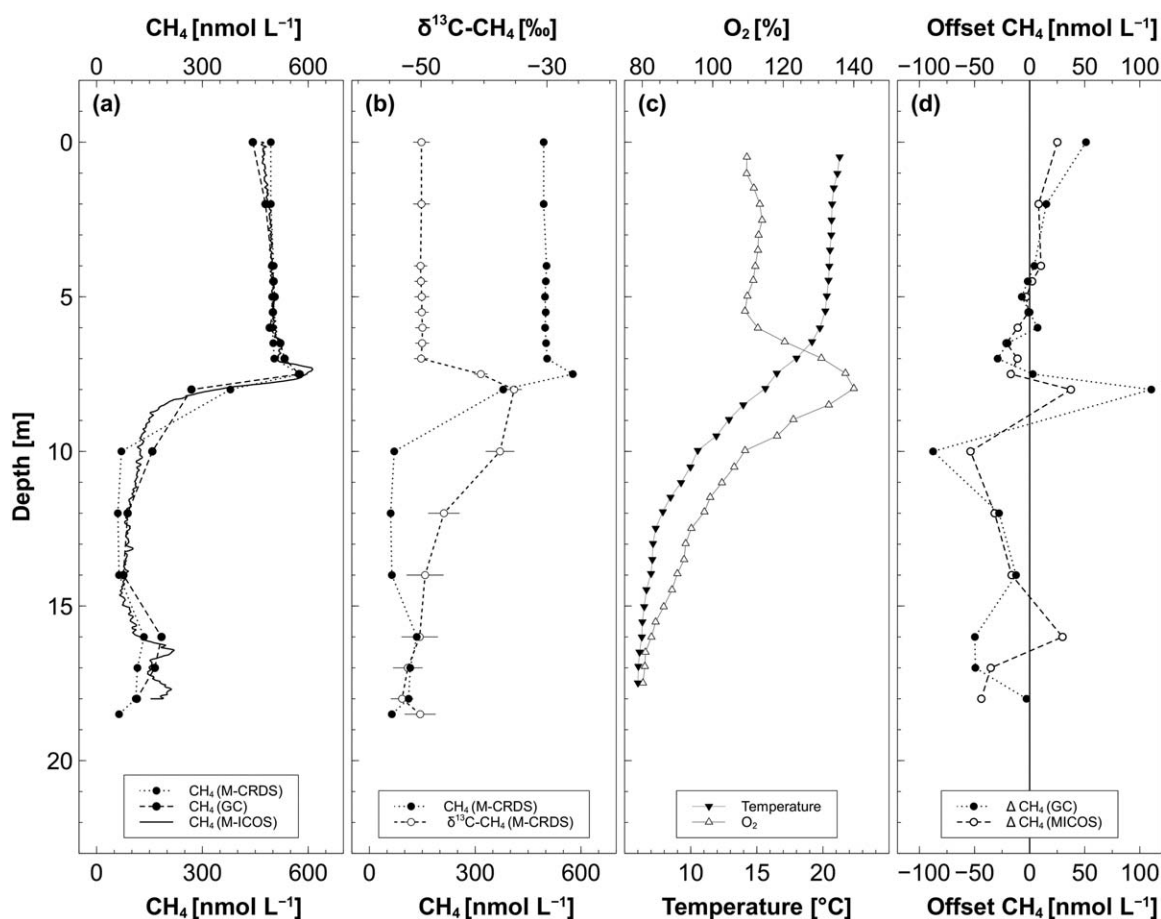
Fig. 5. Depth profiles of different parameters in Lake Stechlin (Germany) in July 2015. Depth profiles for CH₄ were analyzed by M-CRDS, M-ICOS, and GC-FID analysis (**a**), for CH₄ and δ¹³C-CH₄ (**b**) and for temperature and O₂ in July 2015 (**c**). Offset between CH₄ concentrations measured by M-CRDS in comparison with GC-FID (black dots) and M-ICOS (white dots) (**d**). Error bars (1σ) of measurements mainly lie within symbols and reflect the noise within the measurement interval (10 min).

M-CRDS also show a broad range in oxygen concentration (0% up to 130% oxygen saturation) in the water samples. The validation measurements by GC-C-IRMS show no effects of the gas matrix on the stable carbon isotopic values for the natural water samples. However, the analysis of waters with other organics or sulfur containing compounds might strongly affected by interferences on the CRDS measurement that are usually indicated by the in-built ChemDetect™ sensing contaminants in samples. Nevertheless, field measurements will undoubtedly require sampling for validation measurements with GC and GC-C-IRMS for field and long-term measurements.

Field application at Lake Stechlin

The water column of Lake Stechlin (Germany) was analyzed for CH₄ via M-CRDS, M-ICOS, and GC-FID (vie headspace technique) in July 2015 and August 2015 (Fig. 5a). Maximum CH₄ concentrations of M-CRDS (577 nmol L⁻¹), GC-FID (574 nmol L⁻¹), and M-ICOS (613 nmol L⁻¹) at 7 m water depth coincided with the thermocline in Lake Stechlin

(Fig. 5a,c). Epilimnic CH₄ concentrations were constant ($\sim$ 500 nmol L⁻¹), whereas CH₄ decreased at the thermocline and shows constant hypolimnic CH₄ concentrations ($\sim$ 150 nmol L⁻¹). Elevated CH₄ concentrations in the well-oxygenated upper 10 m of the water column were recorded repeatedly in Lake Stechlin and other lakes (Grossart et al. 2011; Tang et al. 2014; McGinnis et al. 2015). The δ¹³C-CH₄ depth profile shows lightest δ¹³C-CH₄ (−35.2‰) at 8 m water depth, whereas epilimnic and hypolimnic δ¹³C-CH₄ were relatively stable at about −50‰ (Fig. 5b). Highest and lowest δ¹³C-CH₄ values of this field campaign are in good agreement with previously published δ¹³C-CH₄ values for depth profiles in Lake Stechlin (Tang et al. 2014). The offset between the CH₄ concentration measured by the M-CRDS in comparison with GC-FID and M-ICOS is shown in Fig. 5d.

The M-CRDS data correlate with the independently measured data by GC-FID and M-ICOS with $R^2 = 0.9946$ and $R^2 = 0.9980$, respectively, which is only slightly lower than the correlation coefficient between M-CRDS and GC-FID analysis via headspace technique during laboratory
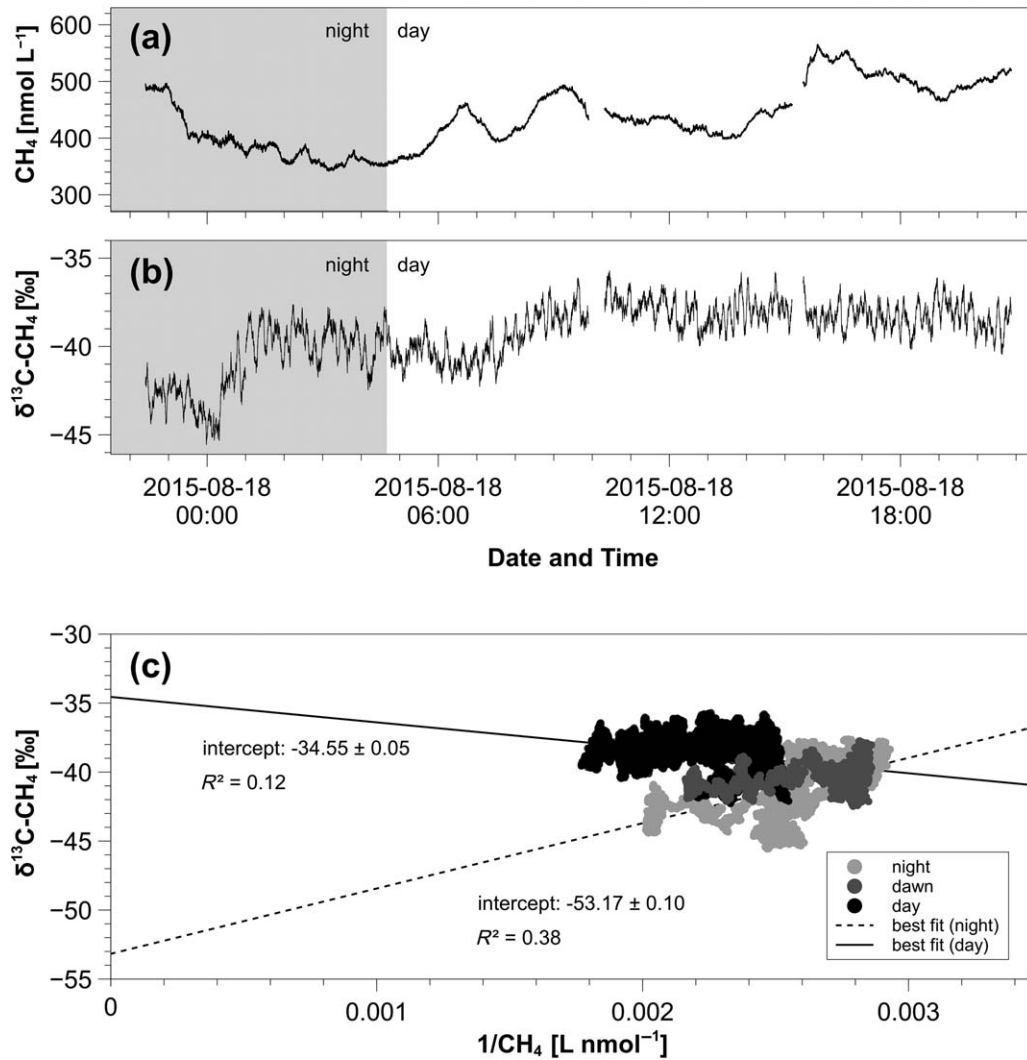
Fig. 6. Results of the 24-h measurement performed at the depth of maximum CH_4 concentration (7 m) at the LakeLab (Lake Stechlin) from 17th August 2015 to 18th August 2015 reveal high temporal variations in CH_4 concentration (**a**) and δ^{13}C-CH_4 (**b**). Night time marked in gray. Keeling-Plot analysis of the 24-h measurement (**c**). The extrapolated intercepts of the best fit in the Keeling plot provide the isotope ratios of the CH_4 sources ($-34.55 \pm 0.05\permil$ and $-53.17 \pm 0.10\permil$). The Keeling plot intercept within the 95% confidence interval was estimated by model II (reduced major axis) regression to obtain the source signature of δ^{13}C-CH_4 (Sokal and Rohlf 1995; Pataki et al. 2003).

calibration ($R^2 = 0.9993$). The mean offset between the CH_4 concentrations measured by M-CRDS and other conventional analytical methods is -5.7 ± 41.6 nmol L^{-1} for GC-FID and -7.8 ± 24.7 nmol L^{-1} for M-ICOS. Epilimnic CH_4 concentration correlate well with the data by GC-FID ($R^2 = 0.9981$) and M-ICOS ($R^2 = 0.9986$), whereas differences between all methods exist in samples below the thermocline. Differences for thermocline samples are best explained by the independent sampling of all three used methods, as the M-ICOS requires its own portable pumping system and the GC samples were taken independently by a hydrocast within routine sampling procedure at the same time. Since the concentration gradient is highest in the thermocline, variations of the sampled water depth directly result in changes in the measured CH_4 concentration. The mean offset of CH_4

concentrations measured by M-CRDS compared to CH_4 concentrations obtained by GC-FID (-28.4 ± 19.0 nmol L^{-1}) and M-ICOS (-19.5 ± 26.2 nmol L^{-1}) is greater at lower concentrations below the thermocline. These deviations from the laboratory calibration of the M-CRDS point out that validation and recalibration by GC-FID measurements are required for future field measurements. However, the presented profile data clearly confirm the suitability of the M-CRDS for in situ analyses of CH_4 concentration and δ^{13}C-CH_4 within surface water and lake environments.

Based on the results of the CH_4 concentration and δ^{13}C-CH_4 profiles by the M-CDRS and the weekly routine sampling procedure for CH_4 concentration at Lake Stechlin, 24-h measurements were performed to detect short-term changes in CH_4 concentration and δ^{13}C-CH_4 at the water

depth of maximum CH_4 concentration (7 m water depth). The presented data are the first demonstrating short-term variations of concentration and δ^{13}C-CH_4 in surface waters (Fig. 6).

The data reveal temporal variations of CH_4 concentration (Fig. 6a) and δ^{13}C-CH_4 (Fig. 6b) at 7 m water depth during the 24-h measurement at Lake Stechlin. CH_4 concentration decreased during night time from 495 nmol L^{-1} to 350 nmol L^{-1} and increased again after sunrise and during the day up to 565 nmol L^{-1}. The δ^{13}C-CH_4 values also showed temporal variations and decreased with decreasing CH_4 concentration from -42‰ to -45‰ and increased rapidly during the early night and after sunrise up to -40‰ and -38‰, respectively. The isotopic values remain rather constant over the day. Temperature differences between the in situ water temperature at the membrane and the temperature at the submersible pump were less than 3.0°C. Effects of the temperature differences on the analyzed CH_4 concentration and δ^{13}C-CH_4 values can be neglected for these temperature ranges.

To determine the δ^{13}C-CH_4 signature of the CH_4 source, the Keeling plot method was applied (Keeling 1958). For the 24-h measurement, the Keeling plot results indicate that CH_4 at 7 m depth (thermocline) might be a mixture of two end members (Fig. 6c). During night time, a ^{13}C depleted CH_4 source was found with a δ^{13}C-CH_4 value of -53‰, whereas the δ^{13}C-CH_4 signature of the CH_4 source during daytime is less depleted in ^{13}C (-35‰). Although the correlation coefficient of the best fit is weak, the calculated results agree very well with the δ^{13}C-CH_4 signatures of the data obtained from the δ^{13}C-CH_4 depth profile as a δ^{13}C-CH_4 value of an approximately -35‰ is found around 8 m, whereas epilimnic and hypolimnic δ^{13}C-CH_4 values are around -50‰ (Fig. 5b).

Temporal variations in CH_4 concentration and δ^{13}C-CH_4 values at Lake Stechlin might therefore be either controlled by local methane production/oxidation or physical variations in the thermocline. Turbulence and internal seiching is a common phenomenon in stratified lakes and reported for Lake Stechlin (Kirillin and Engelhardt 2008; Kirillin et al. 2009; Giling et al. 2016). Lake hydrological dynamics dominated by internal seiches may have partly caused upwelling of colder deep water with lower CH_4 concentration and more negative δ^{13}C-CH_4 (*see* Fig. 6b). However, turbulence sensors were not deployed and, hence, seiche-driven mixing in the thermocline was not measured during our campaign. An alternative explanation for the short-term variations in CH_4 concentration and δ^{13}C-CH_4 values at Lake Stechlin could be both CH_4 production by methanogens or other processes (generating ^{13}C depleted CH_4) and CH_4 oxidation by methanotrophs (generating ^{13}C enriched CH_4) along with photosynthesis (Oswald et al. 2015). Mid-water CH_4 production is a widely occurring phenomena, also previously reported for the oxygen-rich Lake Stechlin water column

(Grossart et al. 2011; Tang et al. 2014). Lateral input of CH_4 from the littoral zone into Lake Stechlin cannot be fully ruled out, despite it was excluded by previous studies, e.g., Tang et al. (2014). Therefore, the high resolution and simultaneous analyses of CH_4 concentration and δ^{13}C-CH_4 values provided by the M-CRDS is critically needed for detailed studies of the origin and fate of mid-water CH_4 in Lake Stechlin (Tang et al. 2016) as the mechanisms and pathways of CH_4 transformation in oxic waters are highly complex and still not fully resolved yet.

Conclusion

The presented CRDS system coupled with a membrane contactor (M-CRDS) enables the sensitive and simultaneous determination of short-term variations of CH_4 concentration and δ^{13}C-CH_4 values in surface waters. Laboratory tests and parallel measurements show a very good comparison of the M-CRDS with GC-FID analyses of CH_4 concentration and IRMS analyses for δ^{13}C-CH_4 values. The good agreement of CH_4 measured simultaneously by M-CRDS, M-ICOS, and GC-FID analysis confirms that the presented M-CRDS method represents an easy and fast to use method, which is ideal to be applied for field work.

The M-CRDS provides the continuous analyses of the dissolved CH_4 concentration in upper surface waters at a very high temporal resolution for flux measurements from aquatic ecosystems to the atmosphere as high temporal variability is not captured by traditional in situ devices or strongly limited by the number of discrete samples. Furthermore, the new instrument is suitable for two-dimensional and three-dimensional mapping of CH_4 concentration and δ^{13}C-CH_4 values. In combination with the continuous in situ analysis of the physical variations within the water column and the biological activity, the M-CRDS will help better understand the complex microbial pathways and transformations of CH_4 in aquatic ecosystems.

However, the investigated method requires further development particularly with respect to the performance stability during measurements of several weeks and months. Although membrane alteration or aging could not be observed during the period of our work, it cannot be ruled out, so that sampling for GC and GC-C-IRMS validation measurements is required. The most appropriate method of validation and recalibration for future application is the analysis of depth profiles in the field since (stratified) lakes cover a broad range of physical and geochemical characteristics as well as CH_4 concentration and δ^{13}C-CH_4. Further development efforts are desirable for calibration and characterization for concentration and isotopic values of CO_2 since the CRDS analyser used in this work allows for simultaneous determination of CO_2 and CH_4 concentration and δ^{13}C values at a very high temporal resolution. Quasi-simultaneous measurements of the concentration and δ^{13}C values of CH_4

and CO_2 will then cover two of the major constituents in carbon cycling and the further application of the M-CRDS in different aquatic environments (e.g., shelves and estuaries) and contribute to a higher temporal and spatial resolution of natural processes representing pathways, sources, and sinks for CO_2 and CH_4 in marine, limnic, and fluvial systems.

References

Abril, G., and N. Iversen. 2002. Methane dynamics in a shallow non-tidal estuary (Randers Fjord, Denmark). Mar. Ecol. Prog. Ser. **230**: 171–181. doi:10.3354/meps230171

Bange, H. W., U. H. Bartell, S. Rapsomanikis, and M. O. Andreae. 1994. Methane in the Baltic and North Seas and a reassessment of the marine emissions of methane. Global Biogeochem. Cycles **8**: 465–480. doi:10.1029/94GB02181

Bastviken, D., L. J. Tranvik, J. A. Downing, P. M. Crill, and A. Enrich-Prast. 2011. Freshwater methane emissions offset the continental carbon sink. Science **331**: 50. doi:10.1126/science.1196808

Botz, R., G. Winckler, R. Bayer, M. Schmitt, M. Schmidt, D. Garbe-Schönberg, P. Stoffers, and J. K. Kristjansson. 1999. Origin of trace gases in submarine hydrothermal vents of the Kolbeinsey Ridge, north Iceland. Earth Planet. Sci. Lett. **171**: 83–93. doi:10.1016/S0012-821X(99)00128-4

Boulart, C., D. P. Connelly, and M. C. Mowlem. 2010. Sensors and technologies for in situ dissolved methane measurements and their evaluation using Technology Readiness Levels. Trends Anal. Chem. **29**: 186–195. doi:10.1016/j.trac.2009.12.001

Brooks, J. M., and W. M. Sackett. 1973. Sources, sinks, and concentrations of light hydrocarbons in the Gulf of Mexico. J. Geophys. Res. **78**: 5248–5258. doi:10.1029/JC078i024p05248

Burke, R. A., T. R. Barber, and W. M. Sackett. 1988. Methane flux and stable hydrogen and carbon isotope composition of sedimentary methane from the Florida Everglades. Global Biogeochem. Cycles **2**: 329–340. doi:10.1029/GB002i004p00329

Bussmann, I., E. Damm, M. Schlüter, and M. Wessels. 2013. Fate of methane bubbles released by pockmarks in Lake Constance. Biogeochemistry **112**: 613–623. doi:10.1007/s10533-012-9752-x

Dando, P. R., J. A. Hughes, Y. Leahy, S. J. Niven, L. J. Taylor, and C. Smith. 1995. Gas venting rates from submarine hydrothermal areas around the island of Milos, Hellenic Volcanic Arc. Cont. Shelf Res. **15**: 913–929. doi:10.1016/0278-4343(95)80002-U

Faure, G. 1986. Principles of isotope geology, 2nd ed. John Wiley and Sons.

Forster, P., and others. 2007. Chapter 2: Changes in atmospheric constituents and in radiative forcing, p. 129–234. *In* S. Solomon, D. Qin, M. Manning, Z. Chen, M. Marquis, K. B. Averyt, M. Tignor, and H. L. Miller [eds.], Climate Change 2007: The physical science basis. Contribution of working group I to the fourth assessment report of the Intergovernmental Panel on Climate Change. Cambridge Univ. Press.

Giling, D. P., and others. 2016. Thermocline deepening boosts ecosystem metabolism: Evidence from a large-scale lake enclosure experiment simulating a summer storm. Glob. Chang. Biol. **23**: 1448–1462. doi:10.1111/gcb.13512

Gonzalez-Valencia, R., F. Magana-Rodriguez, O. Gerardo-Nieto, A. Sepulveda-Jauregui, K. Martinez-Cruz, K. W. Anthony, D. Baer, and F. Thalasso. 2014. In situ measurement of dissolved methane and carbon dioxide in freshwater ecosystems by off-axis integrated cavity output spectroscopy. Environ. Sci. Technol. **48**: 11421–11428. doi:10.1021/es500987j

Grossart, H.-P., K. Frindte, C. Dziallas, W. Eckert, and K. W. Tang. 2011. Microbial methane production in oxygenated water column of an oligotrophic lake. Proc. Natl. Acad. Sci. USA **108**: 19657–19661. doi:10.1073/pnas.1110716108

Gülzow, W., G. Rehder, B. Schneider, J. S. V. Deimling, and B. Sadkowiak. 2011. A new method for continuous measurement of methane and carbon dioxide in surface waters using off-axis integrated cavity output spectroscopy (ICOS): An example from the Baltic Sea. Limnology and Oceanography: Methods **9**: 176–184.

Gülzow, W., G. Rehder, J. Schneider, V. Deimling, T. Seifert, and Z. Tóth. 2013. One year of continuous measurements constraining methane emissions from the Baltic Sea to the atmosphere using a ship of opportunity. Biogeosciences **10**: 81–99. doi:10.5194/bg-10-81-2013

Holgerson, M. A., and P. A. Raymond. 2016. Large contribution to inland water CO_2 and CH_4 emissions from very small ponds. Nat. Geosci. **9**: 222–226. doi:10.1038/ngeo2654

Johnson, J. E. 1999. Evaluation of a seawater equilibrator for shipboard analysis of dissolved oceanic trace gases. Anal. Chim. Acta **395**: 119–132. doi:10.1016/S0003-2670(99)00361-X

Juutinen, S., M. Rantakari, P. Kortelainen, J. T. Huttunen, T. Larmola, J. Alm, J. Silvola, and P. J. Martikainen. 2009. Methane dynamics in different boreal lake types. Biogeosciences **6**: 209–223. doi:10.5194/bg-6-209-2009

Kampbell, D. H., J. T. Wilson, and S. A. Vandegrift. 1989. Dissolved oxygen and methane in water by a GC headspace equilibration technique. Int. J. Environ. Anal. Chem. **36**: 249–257. doi:10.1080/03067318908026878

Keeling, C. D. 1958. The concentration and isotopic abundances of atmospheric carbon dioxide in rural areas. Geochim. Cosmochim. Acta **13**: 322–334. doi:10.1016/0016-7037(58)90033-4

Keppler, F., A. Schiller, R. Ehehalt, M. Greule, J. Hartmann, and D. Polag. 2016. Stable isotope and high precision concentration measurements confirm that all humans produce and exhale methane. J. Breath Res. **10**: 016003. doi:10.1088/1752-7155/10/1/016003

Kirillin, G., and C. Engelhardt. 2008. A mesoscale vortex in a small stratified lake. Environ. Fluid Mech. **8**: 349–366. doi:10.1007/s10652-008-9101-8

Kirillin, G., C. Engelhardt, and S. Golosov. 2009. Transient convection in upper lake sediments produced by internal seiching. Geophys. Res. Lett. **36**: L18601. doi:10.1029/2009GL040064

Kirschke, S., and others. 2013. Three decades of global methane sources and sinks. Nat. Geosci. **6**: 813–823. doi:10.1038/ngeo1955

Lamontagne, R. A., J. W. Swinnerton, and V. J. Linnenbom. 1974. C1-C4 hydrocarbons in the North and South Pacific. Tellus **26**: 71–77. doi:10.1111/j.2153-3490.1974.tb01953.x

Lamontagne, R. A., J. W. Swinnerton, V. J. Linnenbom, and W. D. Smith. 1973. Methane concentrations in various marine environments. J. Geophys. Res. **78**: 5317–5324. doi:10.1029/JC078i024p05317

Lenhart, K., T. Klintzsch, G. Langer, G. Nehrke, M. Bunge, S. Schnell, and F. Keppler. 2015. Evidence for methane production by marine algae *Emiliana huxleyi* and its implication for the methane paradox in oxic waters. Biogeosci. Discuss. **12**: 20323–20360. doi:10.5194/bgd-12-20323-2015

Li, Y., L. Zhan, J. Zhang, and L. Chen. 2015. Equilibrator-based measurements of dissolved nitrous oxide in the surface ocean using an integrated cavity output laser absorption spectrometer. Acta Oceanol. Sin. **34**: 34–41. doi:10.1007/s13131-015-0685-9

Mah, R. A., D. M. Ward, L. Baresi, and T. L. Glass. 1977. Biogenesis of methane. Ann. Rev. Microbiol. **31**: 309–341. doi:10.1146/annurev.mi.31.100177.001521

Maher, D. T., K. Cowley, I. R. Santos, P. Macklin, and B. D. Eyre. 2015. Methane and carbon dioxide dynamics in a subtropical estuary over a diel cycle: Insights from automated in situ radioactive and stable isotope measurements. Mar. Chem. **168**: 69–79. doi:10.1016/j.marchem.2014.10.017

McGinnis, D. F., G. Kirillin, K. W. Tang, S. Flury, P. Bodmer, C. Engelhardt, P. Casper, and H. P. Grossart. 2015. Enhancing surface methane fluxes from an oligotrophic lake: Exploring the microbubble hypothesis. Environ. Sci. Technol. **49**: 873–880. doi:10.1021/es503385d

Nara, H., H. Tanimoto, Y. Tohjima, H. Mukai, Y. Nojiri, K. Katsumata, and C. W. Rella. 2012. Effect of air composition (N_2, O_2, Ar, and H_2O) on CO_2 and CH_4 measurement by wavelength-scanned cavity ring-down spectroscopy: Calibration and measurement strategy. Atmos. Meas. Tech. **5**: 2689–2701. doi:10.5194/amt-5-2689-2012

Noble, R. D., and S. A. Stern. 1995. Membrane separations technology - principles and applications. Elsevier.

Ortiz-Llorente, M. J., and M. Alvarez-Cobelas. 2012. Comparison of biogenic methane emissions from unmanaged estuaries, lakes, oceans, rivers and wetlands. Atmos. Environ. **59**: 328–337. doi:10.1016/j.atmosenv.2012.05.031

Oswald, K., J. Milucka, A. Brand, S. Littmann, B. Wehrli, M. M. M. Kuypers, and C. J. Schubert. 2015. Light-dependent aerobic methane oxidation reduces methane emissions from seasonally stratified lakes. PLoS One **10**: e0132574. doi:10.1371/journal.pone.0132574

Pataki, D. E., and others. 2003. The application and interpretation of Keeling plots in terrestrial carbon cycle research. Global Biogeochem. Cycles **17**: 1022. doi:10.1029/2001GB001850

Paul, D., G. Skrzypek, and I. Forizs. 2007. Normalization of measured stable isotopic compositions to isotope reference scales – a review. Rapid Commun. Mass Spectrom. **21**: 3006–3014. doi:10.1002/rcm.3185

Reeburgh, W. S. 2007. Oceanic methane biogeochemistry. Chem. Rev. **107**: 486–513. doi:10.1021/cr050362v

Reeburgh, W. S. 2013. Global methane biogeochemistry treatise geochemistry, p. 71–94, 2nd ed. **Elsevier**.

Rella, C. W., and others. 2013. High accuracy measurements of dry mole fractions of carbon dioxide and methane in humid air. Atmos. Meas. Tech. **6**: 837–860. doi:10.5194/amt-6-837-2013

Repeta, D. J., S. Ferrón, O. A. Sosa, C. G. Johnson, L. D. Repeta, M. Acker, E. F. DeLong, and D. M. Karl. 2016. Marine methane paradox explained by bacterial degradation of dissolved organic matter. Nat. Geosci. **9**: 884–887. doi:10.1038/ngeo2837

Revelle, R., and H. E. Suess. 1957. Carbon dioxide exchange between atmosphere and ocean and the question of an increase of atmospheric CO_2 during the past decades. Tellus **9**: 18–27. doi:10.1111/j.2153-3490.1957.tb01849.x

Rhee, T. S., A. J. Kettle, and M. O. Andreae. 2009. Methane and nitrous oxide emissions from the ocean: A reassessment using basin-wide observations in the Atlantic. J. Geophys. Res. Atmos. **114**: D12304. doi:10.1029/2008JD011662

Sansone, F. J., M. E. Holmes, and B. N. Popp. 1999. Methane stable isotopic ratios and concentrations as indicators of methane dynamics in estuaries. Global Biogeochem. Cycles **13**: 463–474. doi:10.1029/1999GB900012

Saunois, M., and others. 2016. The global methane budget: 2000–2012. Earth Syst. Sci. Data Discuss. **8**: 697–751. doi:10.5194/essd-8-697-2016

Schlüter, M., and T. Gentz. 2008. Application of membrane inlet mass spectrometry for online and in situ analysis of methane in aquatic environments. J. Am. Soc. Mass Spectrom. **19**: 1395–1402. doi:10.1016/j.jasms.2008.07.021

Schoell, M. 1988. Multiple origins of methane in the earth. Chem. Geol. **71**: 1–10. doi:10.1016/0009-2541(88)90101-5

Snow, N. H., and G. C. Slack. 2002. Head-space analysis in modern gas chromatography. Trends Anal. Chem. **21**: 608–617. doi:10.1016/S0165-9936(02)00802-6

Sokal, R. R., and F. J. Rohlf. 1995. Biometry: The principles and practice of statistics in biological research, 3rd ed. WH Freeman.

Tang, K., D. McGinnis, K. Frindte, V. Brüchert, and H. P. Grossart. 2014. Paradox reconsidered: Methane oversaturation in well-oxygenated lake waters. Limnol. Oceanogr. **59**: 275–284. doi:10.4319/lo.2014.59.1.0275

Tang, K. W., D. F. McGinnis, D. Ionescu, and H.-P. Grossart. 2016. Methane production in oxic lake waters potentially increases aquatic methane flux to air. Environ. Sci. Technol. Lett. **3**: 227–233. doi:10.1021/acs.estlett.6b00150

Thauer, R. K., A.-K. Kaster, H. Seedorf, W. Buckel, and R. Hedderich. 2008. Methanogenic archaea: Ecologically relevant differences in energy conservation. Nat. Rev. Microbiol. **6**: 579–591. doi:10.1038/nrmicro1931

Tranvik, L. J., and others. 2009. Lakes and reservoirs as regulators of carbon cycling and climate. Limnol. Oceanogr. **54**: 2298–2314. doi:10.4319/lo.2009.54.6_part_2.2298

Wankel, S. D., Y. W. Huang, M. Gupta, R. Provencal, J. B. Leen, A. Fahrland, C. Vidoudez, and P. R. Girguis. 2013. Characterizing the distribution of methane sources and cycling in the deep sea via in situ stable isotope analysis. Environ. Sci. Technol. **47**: 1478–1486. doi:10.1021/es303661w

Webb, J. R., D. T. Maher, and I. R. Santos. 2016. Automated, in situ measurements of dissolved CO_2, CH_4, and $\delta^{13}C$ values using cavity enhanced laser absorption spectrometry: Comparing response times of air-water equilibrators. Limnol. Oceanogr.: Methods **14**: 323–337. doi:10.1002/lom3.10092

Weiss, R. F. 1974. Carbon dioxide in water and seawater: The solubility of a non-ideal gas. Mar. Chem. **2**: 203–215. doi:10.1016/0304-4203(74)90015-2

Wiesenburg, D. A., and N. L. Guinasso. 1979. Equilibrium solubilities of methane, carbon monoxide, and hydrogen in water and sea water. J. Chem. Eng. Data **24**: 356–360. doi:10.1021/je60083a006

Wik, M., R. K. Varner, K. W. Anthony, S. MacIntyre, and D. Bastviken. 2016. Climate-sensitive northern lakes and ponds are critical components of methane release. Nat. Geosci. **9**: 99–106. doi:10.1038/ngeo2578

Yamamoto, S., J. B. Alcauskas, T. E. Crozier, J. B. B. Alcauskas, and T. E. Crozier. 1976. Solubility of methane in distilled water and seawater. J. Chem. Eng. Data **21**: 78–80. doi:10.1021/je60068a029

Conflict of Interest

None declared.